An Interdisciplinary Agent-based Evacuation Model: Integrating Natural Environment, Built environment, and Social System for Community Preparedness and Resilience

Chen Chen*[1], Charles Koll[2], Haizhong Wang[3], Michael K. Lindell[4]

*[1]Corresponding Author: College of Engineering, Architecture, and Technology, Oklahoma State University, Stillwater, OK, 74078.
[2]School of Electrical Engineering and Computer Science, Oregon State University, Corvallis, OR 97331.
[3] School of Civil and Construction Engineering, Oregon State University, Corvallis, OR 97331.
[4]Department of Urban Design and Planning, University of Washington, Seattle, WA 98195.

Correspondence to: Chen Chen (chen.chen10@okstate.edu)

Abstract: Previous tsunami evacuation simulations have mostly been based on arbitrary assumptions or inputs adapted from non-emergency situations, but a few studies have used empirical behavior data. This study bridges this gap by integrating empirical decision data from local evacuation expectations surveys and evacuation drills into an agent-based model of evacuation behavior for two Cascadia Subduction Zone (CSZ) communities that would be inundated within 20-40 min after a CSZ earthquake. The model also considers the impacts of liquefaction and landslides from the earthquake on tsunami evacuation. Furthermore, we integrate the slope-speed component from Least-cost-distance to build the simulation model that better represents the complex nature of evacuations. The simulation results indicate that milling time and evacuation participation rate have significant non-linear impacts on tsunami mortality estimates. When people walk faster than 1 m/s, evacuation by foot is more effective because it avoids traffic congestion when driving. We also find that evacuation results are more sensitive to walking speed, milling time, evacuation participation, and choosing the closest safe location than to other behavioral variables. Minimum tsunami mortality results from maximizing the evacuation participation rate, minimizing milling time, and choosing the closest safe destination outside of the inundation zone. This study's comparison of the agent-based model and the Beat-the-Wave (BtW) model finds consistency between the two models' results. By integrating the natural system, built environment, and social system, this interdisciplinary model incorporates substantial aspects of the real world into the multi-hazard agent-based platform. This model provides a unique opportunity for local authorities to prioritize their resources for hazard education, community disaster preparedness, and resilience plans.

1. Introduction

Recent devastating earthquakes and tsunamis have placed immense burdens on their affected communities, such as the 2011 Tohoku tsunami (Mori et al., 2011), the 2009 American Samoa tsunami (Lindell et al., 2015), and the 2018 Indonesia Sulawesi tsunami (Sassa and Takagawa, 2019). Due to a small evacuation time window between the end of earthquake shaking and the arrival of the first tsunami wave, a high level of evacuation efficiency is essential for minimizing the loss of life in low-lying coastal communities subject to local tsunamis (Wang et al., 2016; Raskin and Wang, 2017). To reduce evacuation clearance time (the sum of authorities' decision time, warning dissemination time, households' preparation time, and evacuation travel time) and thus maximize survival rates during tsunamis, researchers and practitioners have developed evacuation simulations to support decision-making, public education, and community emergency planning and management.

1.1. Previous ABMSs for Earthquake and Tsunami Evacuation

Agent-based modeling and simulation (ABMS), as a type of highly effective computational simulation model, has been applied to many research fields (Mas et al., 2013; Mostafizi et al., 2019a). The unique characteristics of ABMS include a bottom-up structure and ability to model heterogeneous agents and their interactions with other agents. These unique characteristics meet the needs of disaster evacuation simulation (Gilbert, 2007). The bottom-up structure provides an opportunity to analyze how changes in evacuation behavior affect the overall evacuation result. One concern about using ABMS is the computational expense, but this is less of an issue as computing costs continue to decrease (Lindell et al., 2019). This increase in computational power has allowed disaster researchers to apply ABMS to 1) simulate evacuation in large-scale communities and 2) integrate different layers of data to comprehensively analyze evacuation with consideration of interactions between the natural environment, built environment, and social system. Table 1 identifies recent tsunami evacuation ABMS studies and their content.

Table 1: *Recent earthquake and tsunami ABMS studies*

Author / Year	Study Area	Mode	Model Components			Tested Variables
			Natural Environment	Built Environment	Social System	
Chen and Zhan (2008)	San Marcos, TX, USA	Car	N/A	Road network; artificial safe zone	Hypothetical population density; dynamic routing; car following model	Evacuation strategy
Dawson et al. (2011)	Towyn, United Kingdom	Car	Flood inundation	Road network; destination; building	Population distribution; warning time; driving speed; re-route	Warning time; water depth
Karon and Yeh (2011)	Cannon Beach, OR, USA	Walk	Tsunami inundation	Road network; destinations	Warning dissemination; shortest distance; travel speed	Infrastructure retrofitting strategy
Mas et al. (2012)	Arahama village, Japan	Car/Walk	Tsunami inundation	Road network; destinations	Population distribution; evacuation mode; milling time; speed	Evacuation result compared with real event; milling time; destination
Mas et al. (2013)	La Punta, Peru	Car/Walk	Tsunami inundation	Road network; destinations	Population distribution; social status; evacuation mode; milling time; speed	Evacuation result; shelter capacity
Wang et al. (2016)	Seaside, OR, USA	Car/Walk	Tsunami inundation	Road network; destinations	Population distribution; milling time; evacuation mode; speed; route choice	Water depth; milling time; evacuation mode; destination location
Mostafizi et al. (2019a)	Seaside, OR, USA	Walk	Tsunami inundation	Road network; destinations	Population distribution; milling time; speed	Shelter location

In the absence of empirical behavioral data, early-stage evacuation ABMSs were based on arbitrary assumptions, as had been the case for large-scale evacuation models (Lindell and Perry, 1992; Lindell and Prater, 2007). Chen and Zhan (2008) investigated the effectiveness of simultaneous and staged evacuation strategies using an ABMS for San Marcos, Texas. Although this study considered evacuees' car following and dynamic routing behaviors, it was based on many arbitrary assumptions about evacuation behavior, such as homogeneous milling time within a zone, single evacuation mode, evacuees selecting quickest evacuation

route and destination, etc. To reduce reliance on assumptions, Mas et al. (2012) built an evacuation ABMS that included more empirical data from the natural system, built environment, and social system. In this model, agents are characterized by probabilistic distributions of milling time, evacuation mode choice, evacuation destination, and travel speed. By comparing the simulation with data from the 2011 Japanese earthquake and tsunami, the authors concluded that the results from this simulation are consistent with the real event and can be used to analyze evacuation and shelter demand for future events. In 2013, Mas et al. (2013) expanded this ABMS to the city of La Punta, Peru to conduct a vertical and horizontal shelter analysis.

Practitioners and researchers have relied on similarities between the 2011 Japanese earthquake event and the geologically similar Cascadia Subduction Zone (CSZ) to encourage Oregon coastal residents to prepare for local tsunamis. Karon and Yeh (2011) used GIS to build an evacuation ABMS by integrating tsunami inundation, warning transmission, and travel speed to examine the impact of failures of critical infrastructure in Cannon Beach, Oregon. To model heterogeneous agent behaviors, Wang et al. (2016) established a scenario-based tsunami evacuation ABMS for Seaside, Oregon. This study examined the impact of variance in agent behaviors such as milling time, evacuation mode choice, and travel speed. In addition, it also included the impact of a tsunami, but not an earthquake, on the built environment such as damage to streets, bridges, and buildings. A later version of this study, Mostafizi et al. (2019a), used a similar ABMS platform to identify optimum shelter locations considering the population distribution, heterogeneous agent milling time, and walking speed. However, as with previous studies, agents were assumed to evacuate to the closest shelter, which may not accurately represent people's destination choices when threatened by a tsunami.

One common limitation of those evacuation models is that they have evacuation assumptions about the four evacuation time components – authorities' decision delay time, households' warning receipt and decision time, households' evacuation preparation time, and households' evacuation travel time. Warning receipt time, for example, can vary across communities and households. Nagarajan et al. (2012) used an ABMS to test the warning dissemination speed through formal channels transmitted by officials and informal channels transmitted by neighbors. They found that even a small proportion of people who were willing to warn their neighbors has a considerable impact on reducing warning dissemination time. Several previous ABMS studies have also assumed arbitrary probability functions for milling time to represent the variance in evacuation departure times (Mas et al., 2012; Wang et al., 2016; Mostafizi et al., 2019a).

In addition, some recent evacuation simulations have also employed assumptions about the distribution of evacuees' walking speeds. For instance, Wang et al. (2016) and Mostafizi et al. (2019a) assumed a normal distribution of evacuee walking speeds for which the mean was built based on a study of pedestrians walking on streets in non-emergency situations (Knoblauch et al., 1996). This assumption is likely to underestimate travel speeds in a tsunami evacuation and thus overestimate tsunami mortality rates. However, mortality rates might not be overestimated if travel speed is actually reduced by additional barriers such as landslides, liquefaction, and other earthquake disturbances to the evacuation route system.

Failure to consider "shadow evacuation" by residents of areas outside the tsunami inundation

zone can lead to unnecessary evacuation that overwhelms the evacuation route system and impedes travel by people in the inundation zone (Lindell et al., 2019). Instead of assigning a probabilistic distribution to walking speed, Wood and Schmidtlein (2012) used a deterministic hiking function (Tobler, 1993) to define a least cost distance (LCD) model for tsunami evacuation. This hiking function captured the impact of slope on walking speed, but also assumed daily walking conditions rather than emergency conditions. Overall, existing evacuation models have assumed that pedestrians' travel behavior in daily situations represents the corresponding behavior in evacuations, but field or experimental data to confirm this assumption are needed.

Most of the aforementioned studies used Census data to identify agents' evacuation departure locations, so the scenarios assumed people were at home. However, a disaster may happen at any time of the day. To account for the variance in evacuees' locations, Dawson et al. (2011) developed a flood management ABMS to support flood emergency planning and evaluate flood incident management measures. The authors used empirical survey data to integrate warning time and used the National Travel Survey to determine people's locations and travel states (e.g., work, home, or school).

1.2. Other Models for Earthquake and Tsunami Evacuation

Although scenario-based ABMSs have been employed to support evacuation decision-making for entire communities (or large areas), jurisdictions are also interested in the question of how quickly people should evacuate from different sub-areas in a community. Geographers used the LCD method to build the Beat-the-Wave (BtW) model to estimate the maximum travel time that people need to walk out of a tsunami inundation zone (Wood and Schmidtlein, 2012). This model defined the distance cost by two variables – the evacuation route's slope and its land cover. To determine the walking speed, they employed Tobler's hiking function (Tobler, 1993) and the energy cost of the terrain category (Soule and Goldman, 1972). The output of this model provides the spatial distributions of maximum evacuation times to "beat the wave", and can be used for preparedness planning and education. The Oregon Department of Geology and Mineral Industries (DOGAMI) has implemented this model to identify Oregon coastal communities' evacuation route maps and to estimate evacuation travel times (DOGAMI, 2020; Gabel et al., 2019).

Although DOGAMI has used the LCD method because it is relatively easy to calculate and provides reasonable evacuation time estimates (ETEs), it does have some limitations. First, it cannot examine social system variables that influence tsunami evacuation outcomes (such as population distribution, milling time, and the choice of transportation mode, evacuation route, and evacuation destination). Second, it cannot incorporate dynamic travel costs due to crowding or congestion. Agent-based models can overcome those limitations but are sometimes criticized as difficult to implement due to the magnitude of data required. As noted earlier, those data include the distribution of population locations, evacuees' behaviors, and wave-arrival time. However, the ABMS and LCD approaches are not incompatible so a mixed-method approach could be used to better model the complex nature of evacuation (Wood and Schmidtlein, 2012).

1.3. Research Objectives and Questions

The preceding literature review has revealed the need for an evacuation ABMS that can simultaneously consider the natural environment, built environment, and social system to analyze complex evacuation scenarios. Although some studies have incorporated layers from those three systems, most of the data inputs were arbitrary assumptions – a problem that has plagued large scale evacuation modeling (Lindell et al., 2019). To more completely integrate the three systems, this study established an ABMS for tsunami evacuation that integrates 1) the natural environment and its disruptions; 2) the built environment and its disruptions; and 3) the social system, as defined by people's protective actions – especially their evacuation behavior.

Specifically, this ABMS integrates human decisions and evacuation logistics into an ABMS platform using empirical behavior data that were collected through survey questionnaires and evacuation drills from coastal residents facing tsunami threats. This integration operationalizes the Protective Action Decision Model (PADM) (Lindell and Perry, 2012) within an ABMS by incorporating agents' heterogeneous behavior in emergencies, such as 1) evacuation participation; 2) choices of transportation mode, evacuation routes and destinations; and 3) travel speeds. Furthermore, to accurately model the complex nature of evacuation, this ABMS also includes the impact of landslides and liquefaction on the road network during evacuation. Incorporating the essential components of the LCD model (slope and road surface) combines the advantages of the ABMS and BtW models (Wood and Schmidtlein, 2012). ABMS models are implemented for Coos Bay, Oregon and sensitivity analyses are conducted in this study to answer the following questions:

1. How do the evacuation participation rate, milling time, mode choice, destination choice, and travel speed affect mortality rates?
2. Which of these variables have greater impact on mortality rates and which of them can be addressed in tsunami evacuation preparedness?
3. How do the results from the ABMS compare with the results from the BtW model?

This interdisciplinary ABMS can not only serve as an evacuation planning tool for local agencies, but also can be an educational and assessment tool for coastal residents to better prepare for the next threat.

2. Interdisciplinary Tsunami Evacuation ABMS

2.1. Agent-based Modeling Environment

Simulating evacuation is a computationally-intensive problem due to the large scale of the built and natural environments and the complexity of agent behaviors. Therefore, an ABMS typically has a high computational cost when applied to large scale evacuation (Lindell et al., 2019). To overcome this issue, the tsunami evacuation ABMS was built using the Julia programming language, which is a just-in-time compiled language, allowing for high performance and computational speed (Bezanson et al., 2012). The high speed of the Julia language allows researchers to model large communities with detailed heterogeneous agent behaviors. This study's ABMS modeling environment allows users to modify parameters for natural, built, and social systems and also allows stochastic inputs. Figure 1 shows the ABMS visualization and real-time evacuation monitors. The details of the evacuation model environment are discussed in Section 2.3.

2.2. Study Area

A series of CSZ tsunami evacuation studies have used Seaside, OR as a study community because of its high level of vulnerability to local tsunamis (Connor, 2005; Wood et al., 2015; Wang et al., 2016; Chen et al., 2020, 2021). However, other communities that differ from Seaside in their geographic and demographic characteristics should also be examined. This study chose the Coos Bay peninsula as a case study due to four features. First, it has a distinctly vulnerable geography. As Figure 1 indicates, this peninsula is surrounded by bay water on its north, east, and west sides. In addition, its hilly spine in the middle provides ready access to higher ground for evacuation destinations. The bay serves as the second and the sixth largest estuary in Oregon and on the US west coast, respectively (CLW, 2015). Second, this community is located on the southern margin of the CSZ, where the rupture probability is higher and tsunami wave arrival time is shorter than communities farther north (Priest et al., 2014; Chen et al., 2021). Third, the Coos Bay peninsula has a total population of about 26,129, which is the largest population among Oregon coastal communities (United State Census Bureau, 2020). Moreover, a large proportion of the population (about 25%) resides within the inundation zone. Fourth, this community has a high level of social vulnerability due to its demographic characteristics. The local population has a higher percentage of disabled residents and is poorer and less educated than the overall U.S. population (United State Census Bureau, 2020; Chen et al., 2021).
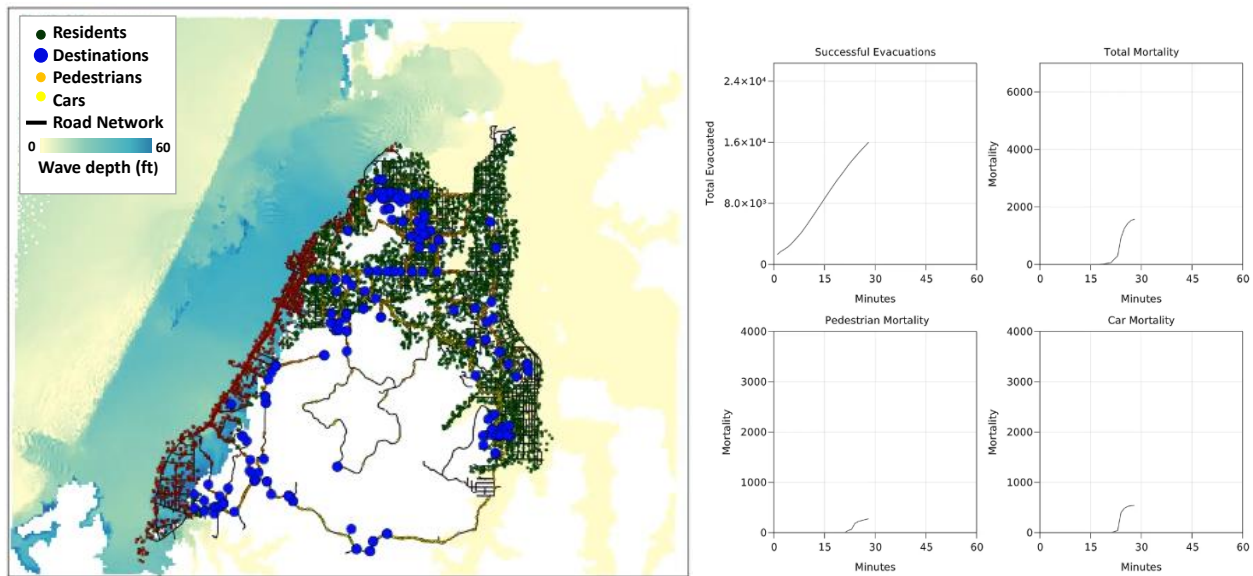
Figure 1: *Simulation model visualization of Coos Bay, Oregon*

2.3. Model Components

To more accurately model tsunami evacuation, this study proposes an ABMS that integrates components of the natural environment, built environment, and social system. Specifically, this ABMS includes the components shown in Table 2.

Table 2: *ABMS components*

System	Component	Description	Data sources
Natural environment	Tsunami inundation layer	Water depth per 30 sec time frame (m)	DOGAMI CSZ near-filed M9 XXL scenario
	Elevation and slope	Use elevation digital model to calculate slope	Oregon 10m Digital Elevation Model (DEM)
	Landslide and liquefaction	Landslide and liquefaction susceptibility to identify disrupted roads	DOGAMI Project O-13-06
Built environment	Road Network	Links	OpenStreetMap & Google Earth
	Non-retrofitted bridges	Manually identified by talking with local authorities	DOGAMI Project O-19-07
Social System	Population distribution	26,000 agents US Census by census block group, then randomly generate along transportation network	US Census
	Evacuation participation	By attributes or proportion (1: evacuate; 0: stay)	Survey
	Milling time	Gamma distributions and a fixed time	Survey
	Mode choice	Proportion, controlled by a parameter	Survey
	Destination choice	Probability distribution on the distance to shelter and use soft-max function to calculate the discrete probability	Survey: distance from home to destination separated by car/foot, gamma distribution
	Evacuation speed – car	IDM model with parameters and a speed limit	Parameter chosen by common scenarios
	Evacuation speed – foot	Evacuation hiking function based on elevation	Evacuation drills
	Route choice	Shortest distance to the destination that agents chose	
	Route diversion	If next intersection is blocked, the agent selects another leg of the intersection, then chooses another destination	

2.3.1. Social System and Agent Behavior

According to the PADM, people make protective action decisions based on environmental/social cues and warnings, which are affected by personal characteristics such as pre-existing beliefs about the hazard, protective actions, and community stakeholders (Lindell and Perry, 2012; Lindell, 2018). The large number of these variables, the difficulty in measuring them, and their heterogeneity among agents makes it difficult to model this part of the evacuation process (Mas et al., 2012). Previous evacuation simulation models (Mas et al., 2012; Wang et al., 2016; Mostafizi et al., 2017, 2019b) assumed that residents evacuate in the most efficient manner (such as selecting the closest shelter), but ignored the heterogeneity in evacuation decisions and actions (Gwynne et al., 1999). One main reason is that these models lacked empirical data on evacuation decisions and actions. To fill that gap, the evacuation model in this study integrates data on people's evacuation decisions and actions that were collected from questionnaire surveys and evacuation drills.

This study employed the PADM as the framework for a mail-based household questionnaire survey that collected data on household evacuation intentions in the Coos Bay area between May and September 2020. There were 258 respondents who returned the questionnaire, which covers their evacuation intentions, expected milling process, and choices of transportation modes and destinations, as well as psychological variables and demographic characteristics. More information can be found in Chen et al. (2021). Probability distributions on these variables are utilized to model the heterogeneous evacuation actions from the data shown in Table 2.

The analyses that follow are based on the ETE model in which the time to clear the risk area is a function of authorities' decision time, warning dissemination time, evacuation preparation time, and evacuation travel time (Lindell et al., 2019). Evacuation preparation time, which is often called "milling" (Wood et al., 2018), has two components – 1) psychological preparation, which involves information seeking and processing to make evacuation decisions; and 2) logistical preparation, which involves performing essential tasks (e.g., packing bags and securing the home) before leaving (Lindell and Perry, 2012). Evacuation travel time is a function of evacuees' choices of transportation mode, evacuation route, and evacuation destination.

Modeling evacuation from a distant tsunami requires data on authorities' decision time and warning receipt time. In the absence of these data, the results of the following analyses

do not apply to distant tsunamis. Modeling evacuation from a local tsunami is simpler because long and strong earthquake shaking is a reliable environmental cue to tsunami onset. Consequently, people who recognize this environmental cue have authorities' decision time and warning dissemination time equal to zero.

Moreover, the following analyses include sensitivity analyses that examine the impact of a plausible range of variation in the input variables on the estimated tsunami mortality rate. As discussed below, these sensitivity analyses can provide useful information for decision making and emergency planning.

Evacuation participation (0: stay; 1: leave) is the protective action that an individual agent selects in response to earthquake shaking or a tsunami warning in this model. According to the Coos Bay community survey, 81% of the respondents intend to evacuate, regardless of their location inside ("compliant evacuees") or outside ("shadow evacuees") of the tsunami inundation zone. Thus, 81% is used as the evacuation participation rate in this model, with a sensitivity analysis on how a change in this rate would impact tsunami mortalities. Evacuees' origins are determined by their locations when an earthquake occurs or a tsunami warning is received. Thus, there is spatial and temporal variability in the distribution of population locations based on factors such as time of day, season, and weather (Wang et al., 2016). This study utilized 2020 US Census (United State Census Bureau, 2020) data to define the origins of 26,363 agents. The scenario examined in this study assumes that all residents are at home, as on a weekend or at night.

The tsunami evacuation intentions questionnaire asked respondents to report how much time they expected it would take them to prepare to evacuate. As shown in equation 1,

$$f(x; \alpha, \beta) = \frac{\beta^\alpha x^{\alpha-1} e^{-\beta x}}{\Gamma(\alpha)} \quad \text{for } x > 0 \quad \alpha, \beta > 0 \tag{1}$$

where x means the milling time and $f(x)$ means the probability of having that milling time for an individual. Applying maximum likelihood estimation to the survey data produced α = 1.659 and β = 6.494 as the estimated parameters of the gamma function for the **milling time** distribution. As Figure 2 indicates, both the Weibull and lognormal distributions provided poorer fits (AIC and BIC) to the data.

Transportation mode choice is a critical factor that affects evacuation success. Agents can choose to evacuate either by foot or by personal vehicle in this model (0: car; 1: foot). In Coos Bay, 70% of the survey respondents reported that they would evacuate by car and only 27% expected to evacuate by foot (Chen et al., 2021).

Destination choice is also obtained from the survey and a probability of choosing a specific destination is assigned to each evacuee based on their distance from the available destinations. A gamma function yields the best goodness-of-fit statistics among the three candidate functions for the destination selection probability, shown in Figure 3. Probability functions were developed separately for evacuation by foot and by car, with maximum likelihood estimation yielding α = 1.920 and β = 500 for evacuation by foot and α = 1.646 and β = 1.745 for evacuation by car.

After agents choose their expected evacuation destinations, the model assigns them to the **shortest route** that is calculated by the A* algorithm (Hart et al., 1968) on the road network. To simulate the behavior of people who encounter an evacuation impediment such as flood on the road while evacuating, agents **divert** to an alternate route. Specifically, when
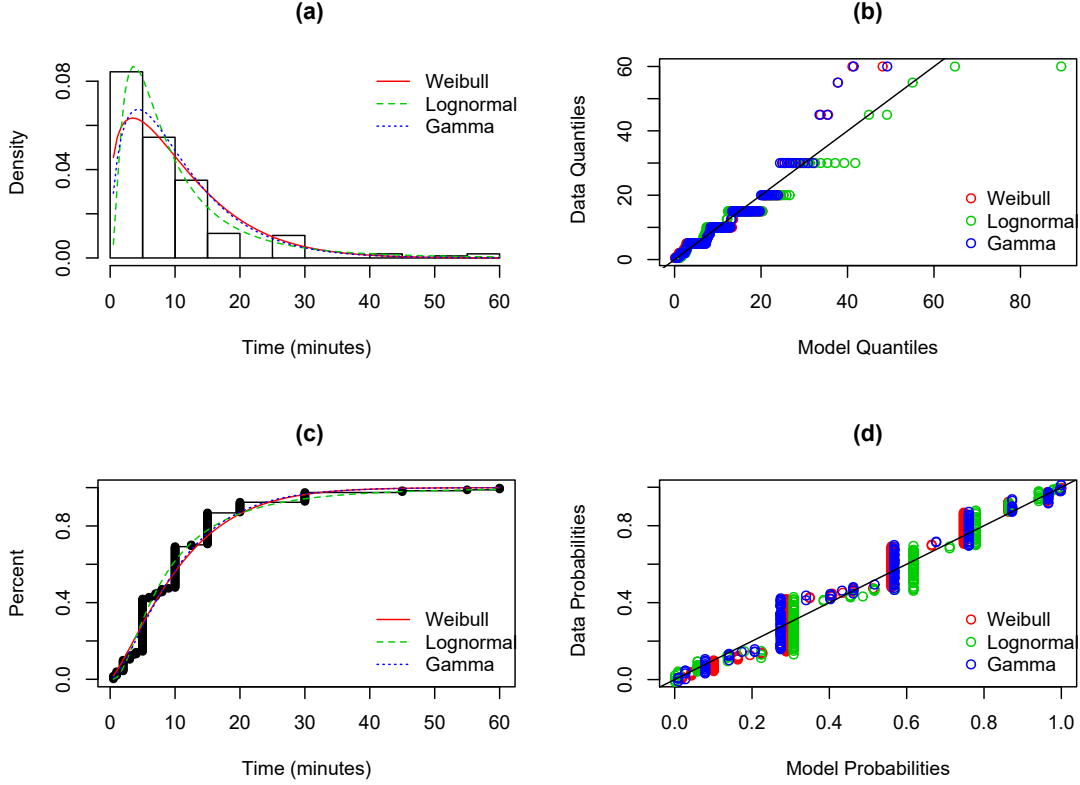
Figure 2: *Expected preparation time from survey data and fitted models: (a) data histogram and probability density function; (b) Quantiles-Quantiles plot; (c) cumulative density function; (d) Probabilities-Probabilities plot.*

agents observe that the next intersection is (inundated by water or damaged by hazards i.e. see section 2.3.3), they select a different leg of the intersection. The model assumes an equal probability of choosing each of the unblocked legs.

The mechanism for assigning a **travel speed** varies, depending on which transportation mode an agent chooses (foot or car). Driving speed is determined by the IDM car following model (Treiber et al., 2000) and the vehicle speed limit on that roadway. Pedestrian walking speed is determined by the slope of the ground on which the pedestrians are walking, through an advanced Hiking Function (Tobler, 1993; Wood and Schmidtlein, 2012). To adjust for differences in walking speeds between daily walking and a tsunami evacuation, we modified the hiking function based on tsunami evacuation drill data that were collected from 2016-2018 (Cramer et al., 2018). In these evacuation drills, 136 evacuees' trajectory data (source: author) were recorded by GNSS embedded mobile devices. The walking speed and slope data were used to modify the hiking function; the modified function is shown in Equation 2.

$$Speed = 1.65 \times e^{(-2.30 \times abs(Slope - 0.004))} \tag{2}$$

To reduce computational cost and optimize simulation speed, the model assigns an average slope to the road segment between each pair of intersections and agents who walk on that segment will have the walking speed that is determined by Equation 2. When conduct-
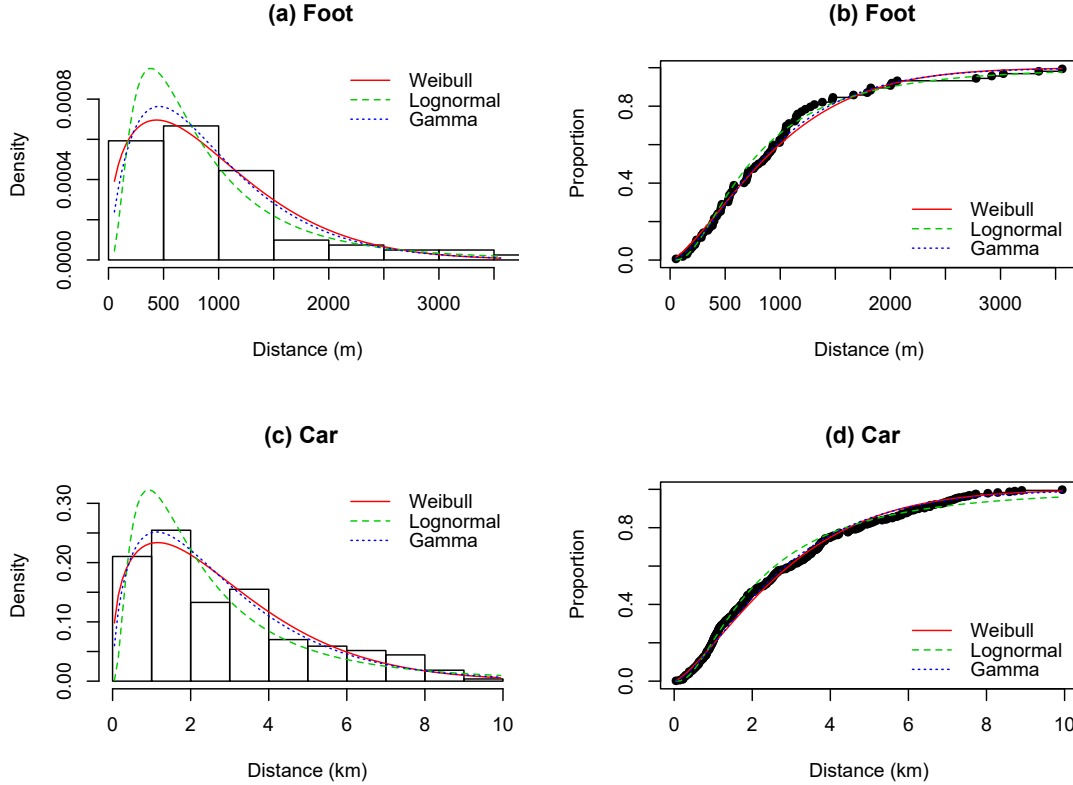
Figure 3: *Intended evacuation destination from survey data and fitted models. Panels (a) and (c) are probability density functions; panels (b) and (d) are cumulative distribution functions.*

ing sensitivity analyses for different values of walking speed, the modified hiking function is disabled when a fixed walking speed is used. Moreover, pedestrian walking speed is reduced based on the conservative value when liquefaction and landslide block a road surface (Schmidtlein and Wood, 2015; Gabel et al., 2019). More details are discussed in Section 2.3.3.

2.3.2. Built Environment

The model's built environment components include the road network and non-retrofitted bridges. The transportation network was obtained from OpenStreetMap (OSM, 2021) and updated manually by the authors based on the 2020 Google Earth satellite image (Google, 2021). All roads are considered to be two-way one-lane streets, as a conservative assumption (Wang et al., 2016). This model also assumes that all agents, whether as pedestrians or in cars, follow the road network to their destinations. Alternative evacuation routes are not included in this simulation, such as swimming across streams or cutting through open fields or parking lots.

Non-retrofitted bridges were located using a study by (Gabel et al., 2019). These bridges are not expected to survive after an M9 CSZ earthquake (Gabel et al., 2019), so they are assumed to be undrivable and unwalkable in this analysis. These bridges are:

- Virginia Ave. on Pony Creek, (1) in Figure 4

332 • Vermont Ave. on Pony Creek, (2) in Figure 4

333 • Broadway Ave. on Pony Creek, (3) in Figure 4

334 *2.3.3. Natural environment*

335 Natural Environment components that are integrated in this model include tsunami inun-
336 dation, terrain elevation and slope, liquefaction susceptibility, and landslide susceptibility.
337 **Tsunami inundation layer:** This model simulates an M9 CSZ earthquake and tsunami
338 using the XXL tsunami inundation model (Witter et al., 2011; Priest et al., 2013). The
339 tsunami inundation layer includes variation in the flow depth and velocity every 30 seconds
340 for each 15-m grid cell from the time the tsunami is generated to eight hours after it reaches
341 the Coos Bay peninsula. The inundation model assumes "bare earth", so the impact of large
342 buildings on water flow was not included.
343 **Topographical elevation and slope:** A 10-m digital elevation model created by U.S.
344 Geological Survey (USGS) (Oregon Geospatial Enterprise Office, 2017) is included as the
345 surface topographical elevation data. In this simulation, elevation data is utilized to calculate
346 the surface slope to inform agents' walking speed using the modified hiking function shown in
347 Equation 2. The slope is calculated by using elevation change (Δy) divided by the Euclidean
348 distance (Δx) change between two points, expressed as (Slope = $\Delta y/\Delta x$).
349 **Landslides and liquefaction:** Evacuation routes can become undrivable and even unwalk-
350 able due to liquefaction, rockfalls, and lateral spreading (Gabel et al., 2019). Susceptibility
351 to both landslide and liquefaction for Coos Bay (Franczyk et al., 2019) is included in this
352 model to estimate which road segments will be disrupted.
353 Landslide susceptibility is calculated based on proximity to landslide deposits, susceptible
354 geologic units, slope angles, and existing landslide inventory. Areas are classified into four
355 susceptibility levels – low, moderate, high, and very high (Burns et al., 2016; Franczyk et al.,
356 2019). Liquefaction susceptibility is calculated from the cohesionless sediments, based on
357 Youd and Perkins (1978); Madin and Burns (2013). Areas are classified into five susceptibility
358 levels – very low, low, moderate, high, and very high. This produces conservative liquefaction
359 levels because it assumes relatively shallow groundwater (Madin and Burns, 2013).
360 Table 3 shows the landslide and liquefaction susceptibility levels that are used in this simu-
361 lation. The spatial areas having a moderate or higher susceptibility level of either landslide
362 or liquefaction are assumed to be disrupted after an M9.0 CSZ earthquake. We consider the
363 moderate level as a threshold to be conservative and realistic. This threshold also has been
364 used by local authorities (Gabel et al., 2019) to build the Coos Bay BtW model. As shown
365 in Figure 4, 54% of the transportation network is exposed to at least a moderate level of
366 liquefaction-landslide susceptibility and 21% is exposed to at least a high level. Thus, the
367 transportation network is likely to be significantly disrupted after an M9.0 earthquake.
368 In this simulation, a street that is predicted to be disrupted by landslide or liquefaction
369 is assigned a rocky or muddy road surface that prevents evacuees from driving through the
370 impediment and makes walking the only feasible transportation mode from that point. Wood
371 and Schmidtlein (2012) adapted a speed conservation value from Soule and Goldman (1972),
372 which is applied to the travel speed of people walking on muddy or rocky terrain surfaces.
373 These values are shown in Table 4.

Table 3: *Landslide and liquefaction susceptibility for network disruption in ABMS*

| | | Landslide Susceptibility | | | |
		Low (0)	Moderate (1)	High (1)	Very high (1)
Liquefaction Susceptibility	Very low (0)	0	$1^\dagger$	1^*	1^*
	Low (0)	0	$1^\dagger$	1^*	1^*
	Moderate (1)	$1^\dagger$	$1^\dagger$	1^*	1^*
	High (1)	1^*	1^*	1^*	1^*
	Very high (1)	1^*	1^*	1^*	1^*

Using a disjunctive decision rule, a spatial area with an index value of at least moderate (54%) or high (21%) level is assumed to be disrupted after an M9 earthquake

†Combined susceptibility level - moderate

*Combined susceptibility level - high

Table 4: *Speed conservation values used in modeling pedestrian walking speed (Wood and Schmidtlein, 2012)*

Feature Type	Speed Conservation Value
Road (Paved)	1
Unpaved Trails	0.9091
Dune Trails (Packed Sand)	0.5556
Muddy Bog	0.5556
Beach (Loose Sand)	0.476

Speed conservation values adapted from Soule and Goldman (1972)

3. Results and Discussion

Figure 5 shows the overall visualization of one run of the model from $0 - 60$ mins after the M9 earthquake. The model assumes that 1) the deformation of subduction zone completes and tsunami is triggered at the source when t = 0 mins; 2) people start the milling process and evacuate either by foot or car; and 3) the first tsunami wave (the highest in a CSZ M9 scenario) arrives in the Barview area (due to being the most westward) at t = $15 - 20$ mins, and starts to inundate to the west shoreline of the peninsula. The first wave arrives at the north side around t = 30 mins and the east side of Coos Bay around t = 40 mins. Most mortalities are observed on roads located in the west shoreline area, followed by the north and east sides.

Two scenarios are examined in this study. **Scenario 1** assumes that the tsunami is the only cause of disaster impacts in the community. Consequently, the road network functions at full capacity until it is inundated by the tsunami waves. Thus, Scenario 1 provides a baseline for assessing the sensitivity of the modeling results to a plausible range of variation in the values of the input variables. **Scenario 2** assumes that an M9 earthquake damages the road network and impedes the evacuation process. According to this scenario, driving may not be possible due to the heavy disruption of roads in large scale landslides, liquefaction, lateral spreading, dropped power lines, debris, and traffic congestion. This assumption has also been applied to previous studies of earthquake and tsunami preparedness in Washington (WGS, 2021), Oregon (DOGAMI, 2020), and California (Cal OES, 2021).
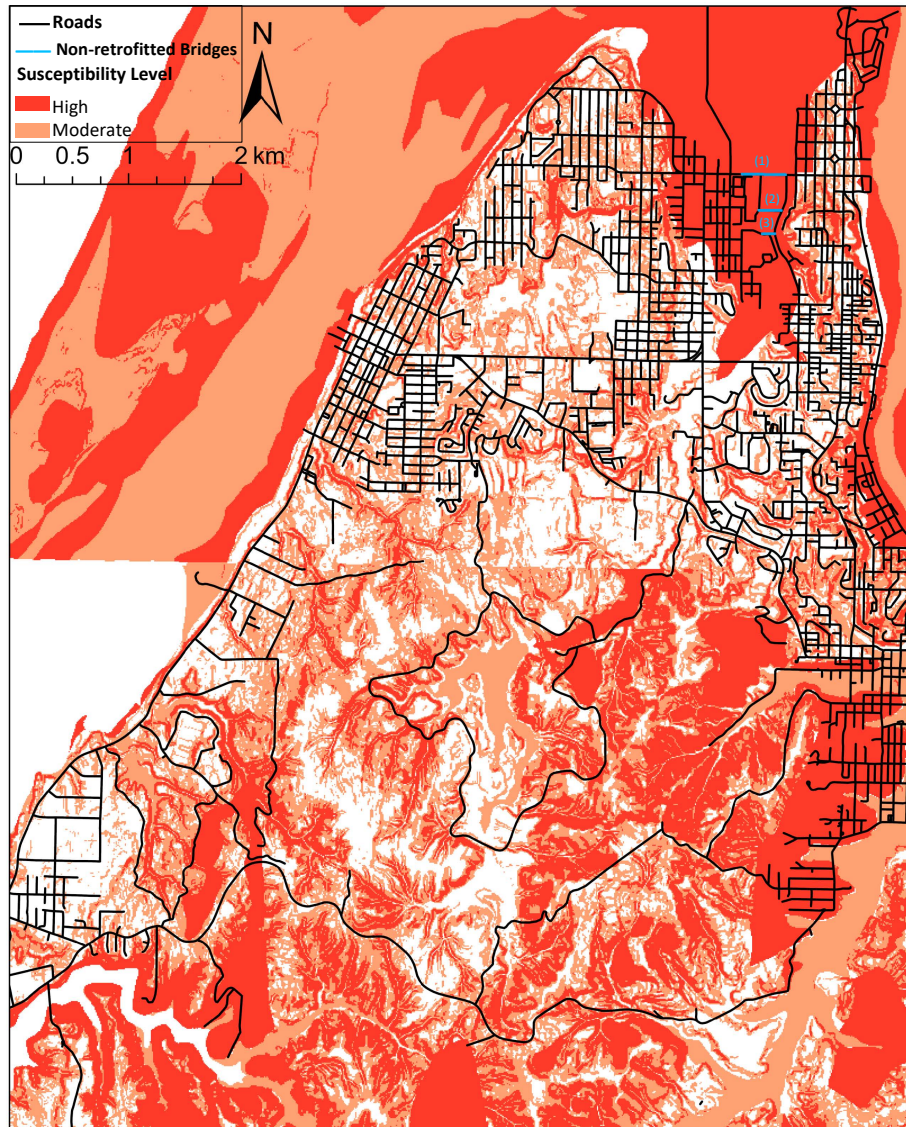
Figure 4: *Coos Bay landslide and liquefaction susceptibility*

3.1. Scenario 1: variable testing with no network disruption

Sensitivity analysis is applied to examine the impact of variation in each model variable on the expected tsunami mortality rate. A Monte Carlo method is employed to capture the probabilistic nature of the inputs and to create an interpretive mean.

3.1.1. Evacuation Decision and Milling Time

Figure 6 shows the sensitivity analysis for the impact of the evacuation participation rate and milling time on mortality rate among the inundation zone population (100% measures only the population live in the inundation zone). Consistent with previous studies (Mas et al., 2013; Wang et al., 2016), these two variables have a significant impact on the estimated mortality rate. The larger the percentage of people who decide to evacuate and the less time people delay before departure, the lower the mortality rate will be. However, the impact of
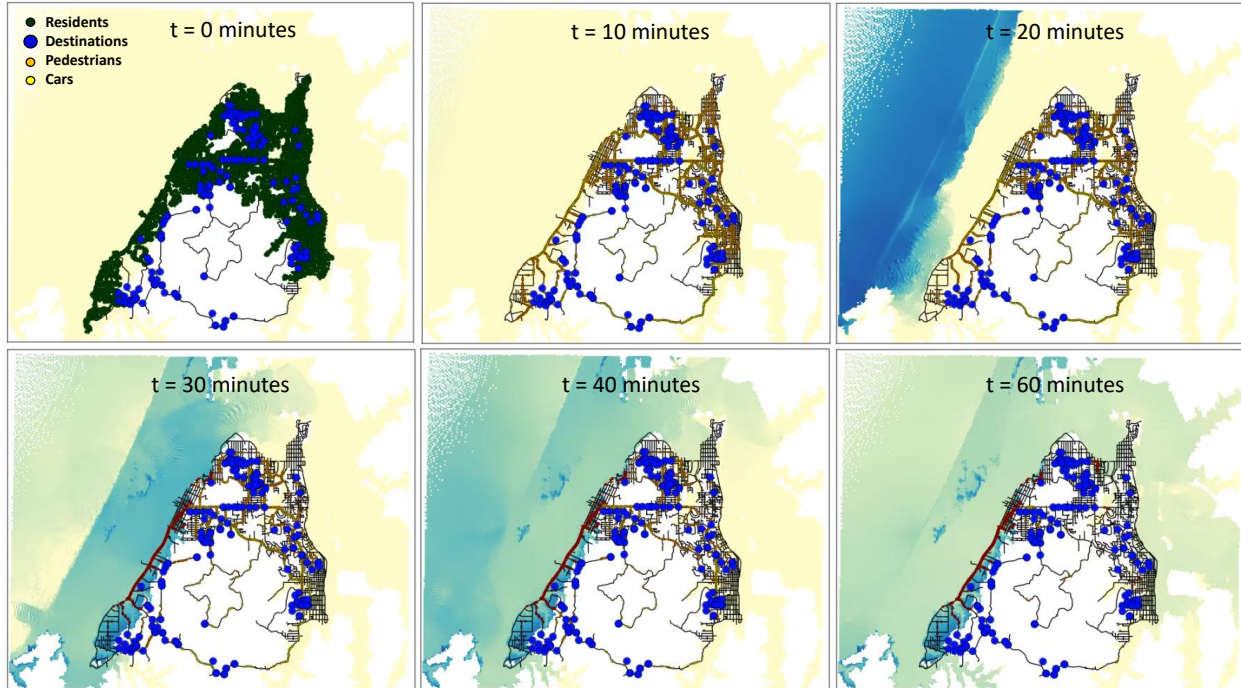
Figure 5: *Model screenshot by time*

milling time on mortality rate is complex, which yields two conclusions.

First, the change in the evacuation participation rate shows a smaller impact when milling time increases. For example, there is no decrease in mortality rate when evacuation participation changes from 10% to 100% at 50 mins of milling time, whereas there is a 88% mortality rate decrease when evacuation participation changes from 10% to 100% at 5 mins of milling time. That is, the effect of decreasing milling time depends on the evacuation participation rate.

Second, the curves that represent high evacuation participation rates in Figure 6 show an "S" shape that indicates the rate of change in mortality is much larger in the middle range of the x-axis from 15 minutes to 25 minutes. Given that the first tsunami wave will arrive on the west side of the Coos Bay peninsula around 15 minutes after the earthquake, the mortality rate will increase substantially as milling time increases past that threshold. Conversely, when milling time is less than 5 minutes and 100% of people decide to evacuate, the curve shows that the mortality rate is extremely low (less than 2%). Thus, the results indicate that reducing the milling time is an important objective for tsunami preparedness programs but it will be most effective when the evacuation participation rate is high.

This result confirms the policy of public authorities on the US west coast (WGS, 2021; DOGAMI, 2020; Cal OES, 2021) to emphasize "Do Not Wait" in their tsunami educational brochures and other outreach products to encourage people to depart as soon as possible after earthquake shaking subsides. Although our simulation findings support this recommendation, gaps remain in the response from local residents. Comparing the survey results of the two variables from Coos Bay (gray areas) with the sensitivity analysis curves shows that the mortality rate is fairly low if based on residents' intended milling time, but it can still be improved by further decreasing milling time and encouraging more people to evacuate.

The same holds true for Crescent City, CA (Chen et al., 2021).
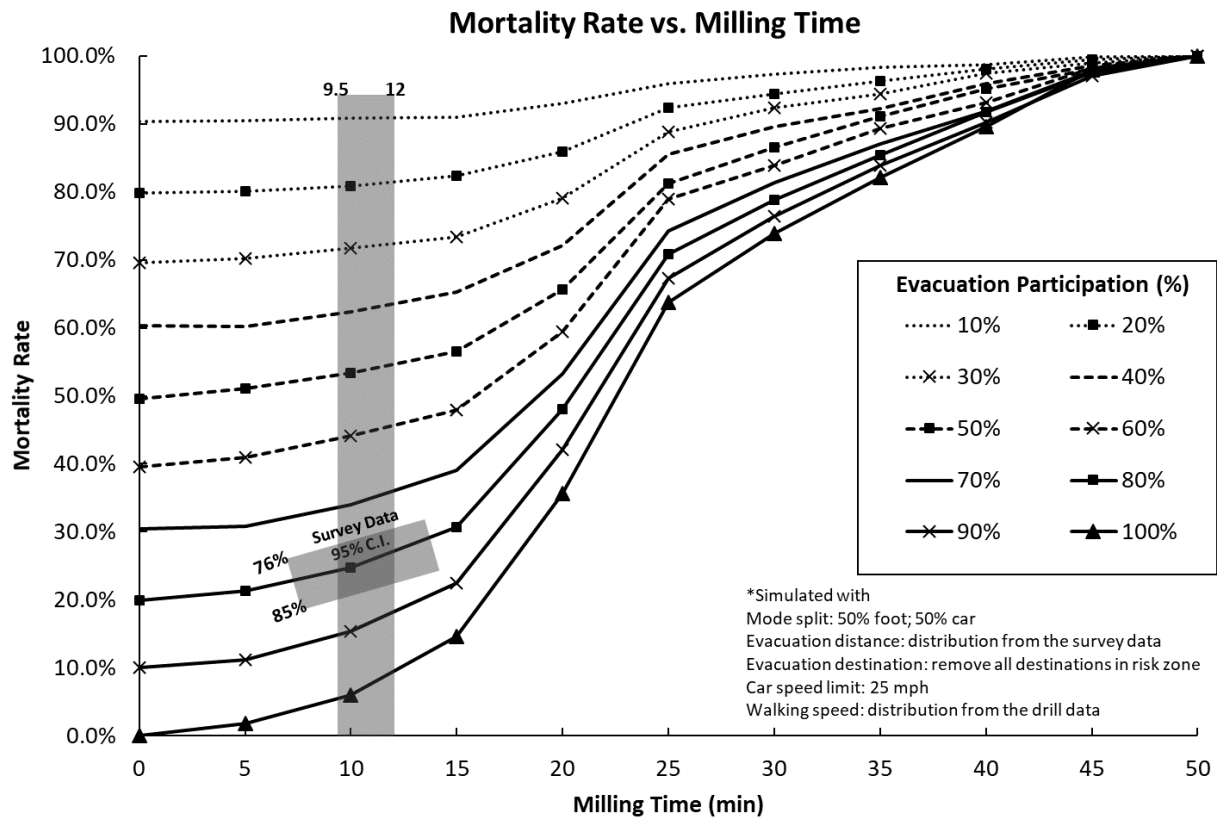
Figure 6: *Estimated mortality rate of the inundation zone population* as a function of milling time and evacuation participation

429

3.1.2. Mode Choice and Walking Speed

Coastal authorities in the CSZ advise evacuating by foot if possible, not only because of potential traffic congestion, but because the road network is likely to be so disrupted that driving may not be feasible to evacuate from a local tsunami. Of course, roads could be flooded by a distant tsunami for which no earthquake shaking could be felt. However, distant tsunamis such as those from the 1964 Alaska and 2011 Japanese tsunamis will take hours to reach the Oregon coast. Consequently, people will have the option of driving when distant tsunamis threaten. Thus, research is needed to examine authorities' recommendation to evacuate by foot and help emergency managers decide when to advise pedestrian evacuation instead of vehicular evacuation. This section analyzes the impact of mode choice and walking speed during evacuation from a local tsunami, and answers the question: Can walking beat driving? If so, in what situations?

Figure 7 shows how walking speed and mode choice influence tsunami mortality estimates. As walking speed increases beyond 1 m/s, the estimated mortality rate decreases as the walking percentage increases. Conversely, as walking speed decreases below 1 m/s, the estimated mortality rate decreases as fewer people choose to walk. This result indicates that if everyone can walk faster than 1 m/s, it is beneficial for more people to evacuate on foot. Given that
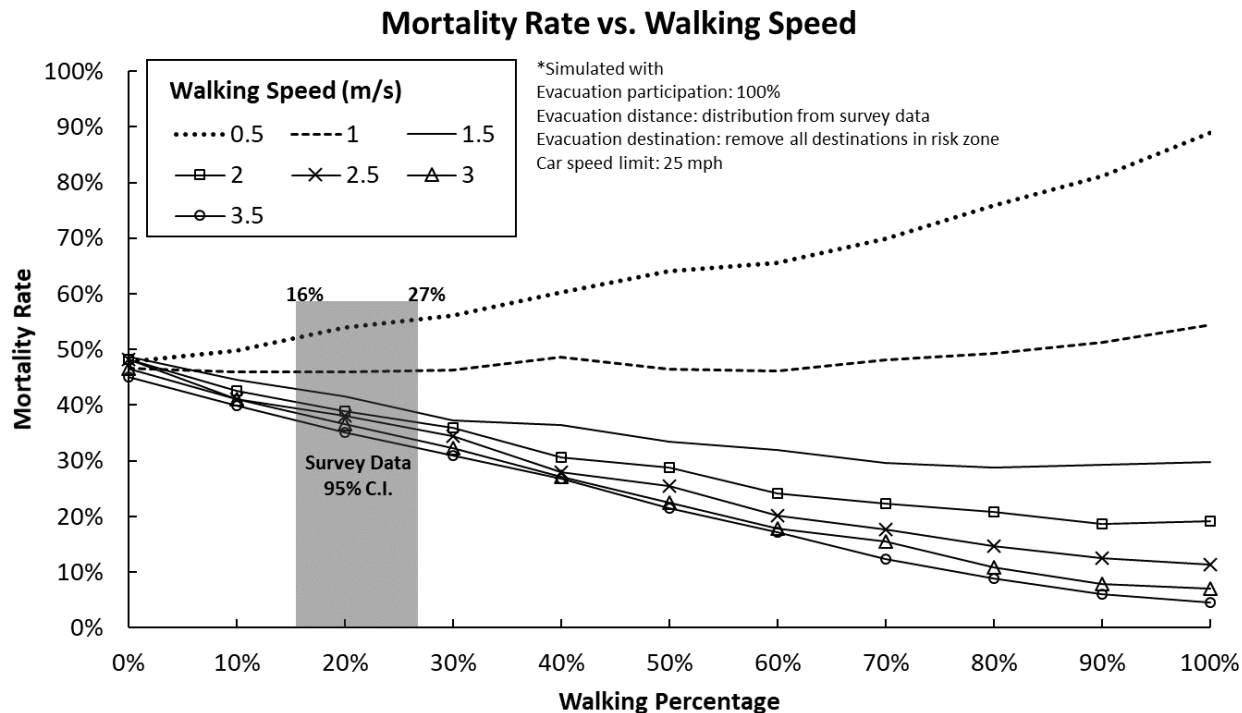
Figure 7: *Mortality rate changes by mode choice and walking speed*

0.91 m/s is a slow walking speed and 1.22 m/s is a moderate walking speed threshold for unimpaired adults (Knoblauch et al., 1996; Langlois et al., 1997; Wood and Schmidtlein, 2012; Fraser et al., 2014), it follows that evacuating on foot is better than evacuating by car if people can walk faster than the slow walking speed threshold. This finding also implies that if people who can walk faster than 1 m/s choose to walk, road network capacity can be saved for mobility impaired people so they can avoid traffic congestion during their evacuation. This is consistent with the finding that 30% evacuation by car and 70% evacuation by foot is the critical threshold for tsunami evacuation in Seaside (Mostafizi et al., 2019b). Similarly, vehicular traffic capacity can be saved for those 30% of the risk area population so they can reach safety in time. However, the question remains: Who should evacuate by car? Even though our finding suggests that most unimpaired people should walk to save traffic capacity for the vulnerable population, risk area residents may behave differently. The survey results show that only 21% of the respondents (95% C.I. 16%–27%) expect to evacuate by foot in Coos Bay (Chen et al., 2021), even though Oregon authorities encourage everyone to do so (DOGAMI, 2020). It is unclear whether this disparity is due to people not having received this recommendation or if they have received it and have chosen not to comply with it.

It should be noted that the results shown in Figure 7 describe the overall picture of evacuation in Coos Bay, but the situation may be different for people living in unique areas that are a long distance from safety, so smaller-scale ABMS or BtW analyses are needed. However, given that the high ground spine in the middle of the Coos Bay peninsula provides a nearby evacuation destination, few people are likely to be in that situation.
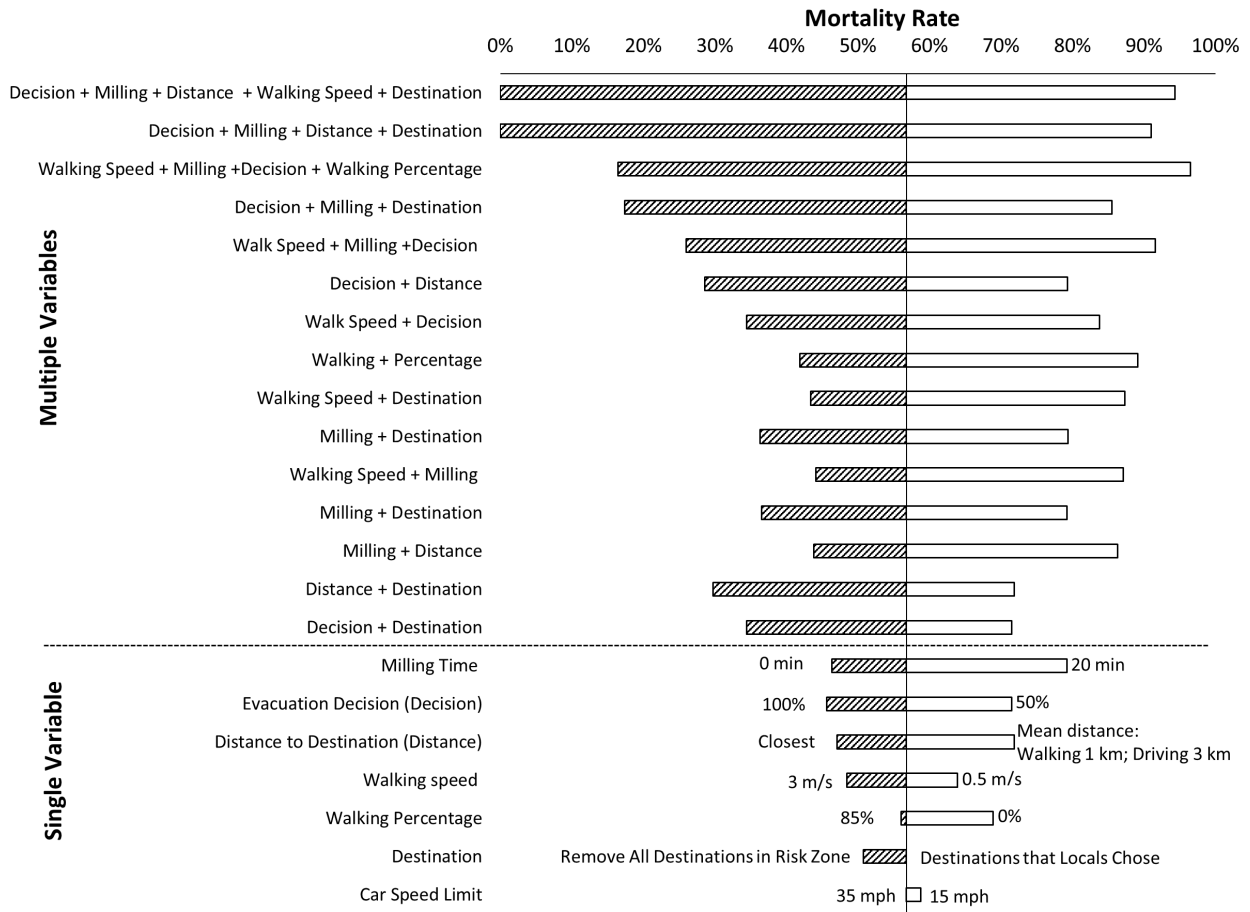
Figure 8: *Impact range of model variables*

3.1.3. Other Variables and Combinations of Variables

Many variables may vary during the evacuation and local authorities need to prioritize resources by deciding which variables or combinations of variables have the greatest impact on expected mortalities. Figure 8 shows the impact on mortality rate of variation in the plausible range of single and multiple variables. The estimated mortality rate for the Coos Bay inundation zone is just over 57% if all of the variables are at their most probable values (the vertical line in the center of the figure) and the bottom bar shows that there is almost no variation in mortality rate as car speed varies from its plausible lower bound (15 mph) to its plausible upper bound (35 mph), whereas it ranges from 45–85% if milling time ranges from 0–20 mins. However, the results show that variation in *Milling Time* and *Evacuation Decision* have the greatest impact on expected mortality when these variables are analyzed individually. This result is consistent with the discussion for Figures 6 and 7 and previous simulation research (Mas et al., 2013; Mostafizi et al., 2019b). Variation in *Distance to Destination* also has a relatively large impact range. Specifically, the lowest mortality occurs when evacuees choose the closest destination and increases when they choose farther destinations. This is because agents tend to spend more time traveling on the roads within the inundation area when they choose farther destinations. This is especially true for

residents living on the west coastal shoreline where the Cape Arago Highway stretches along the shoreline in the inundation zone as the only major road to connect this area to other regions in Coos Bay. When a tsunami strikes, some people who lack knowledge about the inundation area and first wave arrival time may travel on this highway to seek safety farther inland. We observed this "overshooting" behavior in the survey data from both Coos Bay and Crescent City (Chen et al., 2021). The maximum car speed has the lowest impact (2% on mortality rate) of all variables, which is consistent with findings from Mostafizi et al. (2019b) showing the impact range of max car speed is about 2.5 percentage points from 15–35 mph. This finding confirms that driving travel speed is not determined by the maximum speed one can drive at any moment but, rather, by overall road capacity and traffic conditions, which are well-described in traffic flow theory.

The upper panel in Figure 8 shows the impact range of simultaneously changing two or more variables to their lowest plausible levels. Although *Decision + Distance* and *Walking Speed + Decision* have the largest ranges of impact for any pair of variables, there is a similar impact range for other pairs. However, the results show even greater reductions in mortality estimates when more than two variables are at their lowest plausible levels. For example, when optimizing evacuation participation, milling time, and removing destinations in inundation zone, the estimated mortality rate shrinks to less than 20%. When optimizing evacuation participation, milling time, and choosing closest destinations outside of the inundation zone (the second to the top bar), the results show that almost all residents can be saved. Moreover, increasing walking speed from 1.3 m/s to 5 m/s in addition to four other factors (the top bar) produces a similar result. This result indicates that even evacuees who walk slowly are very likely to reach safety in time if they leave immediately for a destination outside of the inundation zone by shortest route. Local authorities should emphasize this finding when deciding what information to communicate in their tsunami preparedness programs.

3.2. Scenario 2: considering network disruption when only walking is available

This section analyzes how network disruptions impact tsunami mortalities when walking is the only option due to road network disruption of the type described in Section 2.3.3. Three scenarios are included in this analysis: 1) when areas with at least moderate landslide-liquefaction susceptibility are disrupted; 2) when only areas with at least high landslide-liquefaction susceptibility are disrupted; and 3) when there is no network disruption. As Figure 9 indicates, there is a nonlinear decrease in estimated mortality as walking speed increases for all three scenarios. That the slopes of the lines decrease as walking speed increases indicates that the marginal effect of changing walking speed on estimated mortality is larger in the lower part of the range. For example, an increase from 0.5 m/s (slow walk) to 1 m/s (normal walk) would yield a 24 percentage point decrease in estimated mortality. However, when areas of the road network with at least moderate susceptibility are disrupted, the model shows an increase of 9 percentage points in estimated mortality for all walking speeds in the 0.25–1.5 m/s range, compared with the results for no disruption. When only areas with a high level of susceptibility are disrupted, there is only a slight decrease in estimated mortality, compared with the results for moderate disruption. When walking speed increases to 1.5 m/s (fast walk), the impact of network disruption is minimal and almost all people can successfully evacuate. Previous research on Seaside (Wang et al., 2016) found a similar decrease to the one shown in Figure 9. In their study, estimated mortality decreased

to zero when walking speed increased to 2 m/s when there was no disruption. This similarity suggests that similar results would be found in communities whose inundation zones have similarly ready access to high ground.

The results from the ABMS is consistent with the results from the BtW model established for Coos Bay (Gabel et al., 2019) with slight differences shown in Figure 9. The similarity between the two models is likely due to the similar input parameters. For example, the survey data from Coos Bay suggest a gamma distribution ($\alpha = 1.66$, $\beta = 6.49$) to model milling time with mean $= 10.77$ mins; this distribution is used in the ABMS to define agents' milling time, whereas the BtW model assumes a 10 min fixed milling time (Gabel et al., 2019). The slight differences between the two results are also due to the inputs of the two models: the parameters are stochastic in the ABMS but fixed in the BtW model, even though they have similar means. The resulting similarities provide convergent validation of the two models, so that jurisdictions can choose either one depending on the purpose of study. The two models should not be considered mutually exclusive; a mixed-method model could be applied to more accurately assess evacuation results (Wood and Schmidtlein, 2012). However, the convergence is based on the assumption that the survey respondents have accurate estimates of the time it takes them to prepare to leave. This is probably the case for those who have "grab and go" kits but is less likely for those who do not. In particular, research on the *planning fallacy* suggests that the survey data are underestimates for some respondents (Buehler et al., 2010).
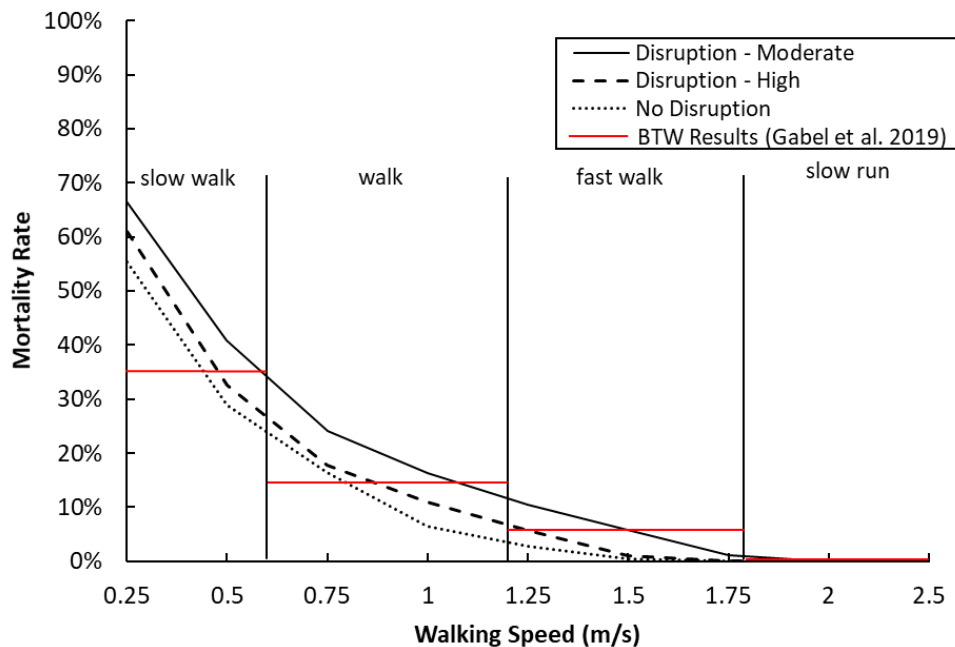
Figure 9: *Network disruption impact: ABMS and BtW model result comparison*

4. Conclusion

Although previous tsunami evacuation simulations have considered the natural environment, built environment, and social system in their models, many data inputs were arbitrary

assumptions or adapted from studies of non-emergency situations, so the simulation results may not accurately reflect what would happen in a tsunami evacuation. The present study addressed this limitation by integrating behavioral data from community surveys into an ABMS for a CSZ community. Four distinct contributions of this study are: 1) using the PADM as a guide for collecting data on people's expected evacuation behavior and the integration of these data into the ABMS; 2) using empirical data from evacuation drills to refine people's evacuation walking speeds; 3) considering the impact of earthquake-caused landslides and liquefaction on tsunami evacuation as a substantial aspect of the multi-hazard situation; and 4) integrating the LCD component from the Wood and Schmidtlein (2012) BtW model – walking speed conservation by surface terrain and slope. By integrating the natural environment, built environment, and social system, this model incorporates substantial aspects of the real world into a multi-hazard ABMS. The simulation results indicate that milling time and evacuation participation have significant non-linear impacts on tsunami mortality estimates, which is consistent with Wang et al. (2016). The impact of milling time on the mortality rate shows an "S" curve, so the impact of milling time on estimated mortality varies the most when evacuation participation is highest. When comparing which transportation mode people should take, the model result shows that more people can reach safety in time when they choose to walk and are able to walk faster than 1 m/s (slow walk). These findings support an important point for tsunami education programs in CSZ communities. Since the majority of Coos Bay respondents expected to evacuate by car instead of on foot, local authorities need to emphasize the need for pedestrian evacuation in their tsunami education programs.

This study also makes a significant contribution to understanding the impact of different variables on tsunami mortality estimates. Evacuation success is more sensitive to walking speed, milling time, evacuation participation, and choice of the closest safe location than to other variables. Consistent with previous research, car speed has little impact on evacuation results. Further, this study also compared the sensitivities of different combinations of variables. Tsunami mortality estimates are minimized when maximizing evacuation participation, minimizing milling time, and choosing the closest safe destination outside of the inundation zone. Furthermore, to validate this model, this study compared the ABMS results with the BtW model results from Gabel et al. (2019) for Coos Bay. Even though the BtW model relies on a Geographical Information System rather than an ABMS, this study's preliminary comparison indicates a good match between results from the two models.

Finally, every study has limitations, as does this one. The agent decision and behavior is based on survey data and drill data, rather than data from an actual tsunami evacuation, so the results might not accurately predict the response to an actual tsunami. Future research should investigate 1) the impact of more complex agent-agent interactions, such as leader-follower behaviors and grouping behaviors (Chen et al., 2020), as well as car abandonment (Wang et al., 2016); 2) the impact of building damage from earthquake before tsunami (Gomez-Zapata et al., 2021); 3) authorities' decision and warning dissemination processes for distant tsunamis; and 4) validation of the model using data from actual tsunami evacuations.

Code/Data availability

The codes and data models used in this paper have been made available in open repositories. Reader can also contact authors for details.

Competing interests

All authors declare that they have no conflict of interest.

Author contribution

Chen Chen: method and model development, analysis, and writing. Charles Koll: model development and revising. Haizhong Wang and Michael Lindell: method development, analysis, and revising.

Acknowledgement

The authors would like to acknowledge the funding support from the National Science Foundation through grants CMMI #1563618, #1826407, and #1826455. Any opinions, findings, and conclusion or recommendations expressed in this research are those of the authors and do not necessarily reflect the view of the funding agency. We are also thankful to Laura Gabel and Jonathan Allan from DOGAMI for providing tsunami inundation model, as well as their constructive suggestions and advises. This project was approved by the Oregon State University Human Research Protection Program (HRPP) and Institutional Review Board (IRB) and follows the regulations to protect participants, with project reference number 0489.

References

Bezanson, J., Karpinski, S., Shah, V. B., Edelman, A., Sep. 2012. Julia: A Fast Dynamic Language for Technical Computing. arXiv:1209.5145 [cs].
URL http://arxiv.org/abs/1209.5145

Buehler, R., Peetz, J., Griffin, D., Jan. 2010. Finishing on time: When do predictions influence completion times? Organizational Behavior and Human Decision Processes 111 (1), 23–32.
URL https://linkinghub.elsevier.com/retrieve/pii/S0749597809000715

Burns, W. J., Mickelson, K. A., Madin, I. P., 2016. Landslide Susceptibility Overview Map of Oregon. Tech. Rep. REPORT O-16-02, Oregon Department of Geology and Mineral Industries.
URL https://www.oregongeology.org/pubs/ofr/p-O-16-02.htm

Cal OES, 2021. How to Survive a Tsunami. Tech. rep., California Governor's Office of Emergency Services.
URL https://www.conservation.ca.gov/cgs/Documents/Tsunami/How-to-Survive-a-Tsunami.pdf

Chen, C., Buylova, A., Chand, C., Wang, H., Cramer, L. A., Cox, D. T., Jun. 2020. Households' intended evacuation transportation behavior in response to earthquake and tsunami hazard in a Cascadia Subduction Zone city. Transportation Research Record 2674 (7).
URL http://journals.sagepub.com/doi/10.1177/0361198120920873

Chen, C., Lindell, M. K., Wang, H., 2021. Tsunami preparedness and resilience in the Cascadia Subduction Zone: A multistage model of expected evacuation decisions and mode choice. International Journal of Disaster Risk Reduction 59, 102244.
URL https://www.sciencedirect.com/science/article/pii/S2212420921002107

Chen, X., Zhan, F. B., Jan. 2008. Agent-based modelling and simulation of urban evacuation: relative effectiveness of simultaneous and staged evacuation strategies. Journal of the Operational Research Society 59 (1), 25–33.
URL https://www.tandfonline.com/doi/full/10.1057/palgrave.jors.2602321

CLW, 2015. Geographic Features of the Coos Estuary and Lower Coos Watershed. Tech. rep., The Communities, Lands & Waterways Data Source.
URL http://www.partnershipforcoastalwatersheds.org/wordpress/wp-content/uploads/2015/08/FINAL-Geographic-Features-Data-Summary.pdf

Connor, D., 2005. Outreach assessment: How to implement an effective tsunami preparedness outreach program. Tech. rep., State of Oregon Department of Geology and Mineral Industries Open File Report OFR 0-05-10, Portland OR: Nature of the Northwest Information Center.
URL https://www.oregongeology.org/pubs/ofr/O-05-10_onscreen.pdf

Cramer, L., Cox, D. T., Wang, H., 2018. Preparing for The Really Big One: The Importance of Understanding the Local Culture of Resiliency. In: Coastal Heritage and Cultural Resilience. Springer Press, New York, NY, pp. 243–264.

Dawson, R. J., Peppe, R., Wang, M., Oct. 2011. An agent-based model for risk-based flood incident management. Natural Hazards 59 (1), 167–189.
URL http://link.springer.com/10.1007/s11069-011-9745-4

DOGAMI, 2020. Larger-Extent Evacuation Brochures. Tech. rep., State of Oregon Department of Geology and Mineral Industries.
URL https://www.oregongeology.org/tsuclearinghouse/pubs-evacbro.htm

Franczyk, J. J., Burns, W. J., Calhoun, N. C., 2019. Statewide Landslide Information Database for Oregon (SLIDO) Release 4.0. Tech. Rep. ORS 516.030, Oregon Department of Geology and Mineral Industries.
URL https://www.oregongeology.org/slido/data.htm

Fraser, S. A., Wood, N. J., Johnston, D. M., Leonard, G. S., Greening, P. D., Rossetto, T., Nov. 2014. Variable population exposure and distributed travel speeds in least-cost tsunami evacuation modelling. Natural Hazards and Earth System Sciences 14 (11),

666 2975–2991.
667 URL `https://nhess.copernicus.org/articles/14/2975/2014/`

668 Gabel, L. L. S., O'Brien, F. E., Bauer, J. M., Allan, J. C., 2019. Tsunami evacuation
669 analysis of communities surrounding the Coos Bay estuary: Building community
670 resilience on the Oregon coast. Tech. Rep. O-19-07, Oregon Department of Geology and
671 Mineral Industries.
672 URL `https://www.oregongeology.org/pubs/ofr/p-O-19-07.htm`

673 Gilbert, N., 2007. Agent-Based Models (Quantitative Applications in the Social Sciences).
674 SAGE Publication Ltd.

675 Gomez-Zapata, J. C., Brinckmann, N., Harig, S., Zafrir, R., Pittore, M., Cotton, F.,
676 Babeyko, A., Nov. 2021. Variable-resolution building exposure modelling for earthquake
677 and tsunami scenario-based risk assessment: an application case in Lima, Peru. Natural
678 Hazards and Earth System Sciences 21 (11), 3599–3628.
679 URL `https://nhess.copernicus.org/articles/21/3599/2021/`

680 Google, 2021. Google Earth.
681 URL `https://www.google.com/earth/versions/`

682 Gwynne, S., Galea, E. R., Owen, M., Lawrence, P. J., Filippidis, L., 1999. A review of the
683 methodologies used in evacuation modelling. Fire and Materials 23 (6), 383–388.

684 Hart, P., Nilsson, N., Raphael, B., 1968. A Formal Basis for the Heuristic Determination of
685 Minimum Cost Paths. IEEE Transactions on Systems Science and Cybernetics 4 (2),
686 100–107.
687 URL `http://ieeexplore.ieee.org/document/4082128/`

688 Karon, J., Yeh, H., 2011. Comprehensive Tsunami Simulator for Cannon Beach, Oregon.
689 Tech. rep., City of Cannon Beach.
690 URL `https://www.ci.cannon-beach.or.us/sites/default/files/`
691 `fileattachments/demo_emergency_management/page/18691/cannon-beach-`
692 `tsunami-final-report-may-2011.pdf`

693 Knoblauch, R. L., Pietrucha, M. T., Nitzburg, M., Jan. 1996. Field studies of pedestrian
694 walking dpeed and start-up time. Transportation Research Record 1538 (1), 27–38,
695 publisher: SAGE Publications Inc.
696 URL `https://doi.org/10.1177/0361198196153800104`

697 Langlois, J. A., Keyl, P. M., Guralnik, J. M., Foley, D. J., Marottoli, R. A., Wallace, R. B.,
698 Mar. 1997. Characteristics of older pedestrians who have difficulty crossing the street.
699 American Journal of Public Health 87 (3), 393–397.
700 URL `http://ajph.aphapublications.org/doi/10.2105/AJPH.87.3.393`

701 Lindell, M. K., 2018. Communicating imminent risk. In: Rodríguez H., Donner W., Trainor
702 J. (eds) Handbooks of sociology and social research, 2nd Edition. New York: Springer,
703 pp. 449–477.

Lindell, M. K., Murray-Tuite, P., Wolshon, B., Baker, E. J., 2019. Large-Scale Evacuation: The Analysis, Modeling, and Management of Emergency Relocation from Harzardous Areas. Routledge, p. 22.

Lindell, M. K., Perry, R. W., 1992. Behavioral foundations of community emergency planning. Behavioral foundations of community emergency planning. Hemisphere Publishing Corp, Washington, DC, US, pages: xi, 309.

Lindell, M. K., Perry, R. W., Apr. 2012. Theoretical modifications and additional evidence: the protective action decision model. Risk Analysis 32 (4), 616–632.
URL http://doi.wiley.com/10.1111/j.1539-6924.2011.01647.x

Lindell, M. K., Prater, C. S., Mar. 2007. Critical Behavioral Assumptions in Evacuation Time Estimate Analysis for Private Vehicles: Examples from Hurricane Research and Planning. Journal of Urban Planning and Development 133 (1), 18–29.
URL http://ascelibrary.org/doi/10.1061/%28ASCE%290733-9488%282007%29133%3A1%2818%29

Lindell, M. K., Prater, C. S., Gregg, C. E., Apatu, E. J., Huang, S.-K., Wu, H. C., Jun. 2015. Households' immediate responses to the 2009 American Samoa earthquake and tsunami. International Journal of Disaster Risk Reduction 12, 328–340.
URL https://linkinghub.elsevier.com/retrieve/pii/S2212420915000266

Madin, I. P., Burns, W. J., 2013. Ground motion, ground deformation, tsunami inundation, coseismic subsidence, and damage potential maps for the 2012 Oregon Resilience Plan for Cascadia Subduction Zone Earthquakes. Tech. Rep. REPORT O-13-06.
URL https://www.oregongeology.org/pubs/ofr/p-O-13-06.htm

Mas, E., Adriano, B., Koshimura, S., Mar. 2013. An integrated simulation of tsunami hazard and human evacuation in La Punta, Peru. Journal of Disaster Research 8 (2), 285–295.
URL https://www.fujipress.jp/jdr/dr/dsstr000800020285

Mas, E., Suppasri, A., Imamura, F., Koshimura, S., 2012. Agent-based simulation of the 2011 Great East Japan Earthquake/Tsunami evacuation: An integrated model of tsunami inundation and evacuation. Journal of Natural Disaster Science 34 (1), 41–57.
URL
https://www.jstage.jst.go.jp/article/jnds/34/1/34_41/_article/-char/ja/

Mori, N., Takahashi, T., Yasuda, T., Yanagisawa, H., Apr. 2011. Survey of 2011 Tohoku earthquake tsunami inundation and run-up. Geophysical Research Letters 38 (7), n/a–n/a.
URL http://doi.wiley.com/10.1029/2011GL049210

Mostafizi, A., Wang, H., Cox, D., Cramer, L. A., Dong, S., Sep. 2017. Agent-based tsunami evacuation modeling of unplanned network disruptions for evidence-driven resource allocation and retrofitting strategies. Natural Hazards 88 (3), 1347–1372.
URL http://link.springer.com/10.1007/s11069-017-2927-y

743 Mostafizi, A., Wang, H., Cox, D., Dong, S., Mar. 2019a. An agent-based vertical evacuation
744   model for a near-field tsunami: Choice behavior, logical shelter locations, and life safety.
745   International Journal of Disaster Risk Reduction 34, 467–479.
746   URL https://linkinghub.elsevier.com/retrieve/pii/S221242091830918X

747 Mostafizi, A., Wang, H., Dong, S., Nov. 2019b. Understanding the multimodal evacuation
748   behavior for a near-field tsunami. Transportation Research Record 2673 (11), 480–492.
749   URL http://journals.sagepub.com/doi/10.1177/0361198119837511

750 Nagarajan, M., Shaw, D., Albores, P., Aug. 2012. Disseminating a warning message to
751   evacuate: A simulation study of the behaviour of neighbours. European Journal of
752   Operational Research 220 (3), 810–819.
753   URL https://linkinghub.elsevier.com/retrieve/pii/S0377221712001580

754 Oregon Geospatial Enterprise Office, 2017. Oregon 10m Digital Elevation Model (DEM).
755   URL https://spatialdata.oregonexplorer.info/geoportal/details;id=
756   7a82c1be50504f56a9d49d13c7b4d9aa

757 OSM, 2021. OpenStreetMap.
758   URL https://www.openstreetmap.org/

759 Priest, G. R., Witter, R. C., Zhang, Y. J., Wang, K., Goldfinger, C., Stimely, L. L.,
760   English, J. T., Pickner, S. G., Hughes, K. L. B., Wille, T. E., Smith, R. L., 2013.
761   Tsunami inundation scenarios for Oregon. Tech. Rep. Open_file Report O-13-19, Oregon
762   Department of Geology and Mineral Industries.
763   URL https://www.oregongeology.org/pubs/ofr/O-13-19.pdf

764 Priest, G. R., Zhang, Y., Witter, R. C., Wang, K., Goldfinger, C., Stimely, L., Jun. 2014.
765   Tsunami impact to Washington and northern Oregon from segment ruptures on the
766   southern Cascadia Subduction Zone. Natural Hazards 72 (2), 849–870.
767   URL http://link.springer.com/10.1007/s11069-014-1041-7

768 Raskin, J., Wang, Y., Feb. 2017. Fifty-Year Resilience Strategies for Coastal Communities
769   at Risk for Tsunamis. Natural Hazards Review 18 (1), B4016003.
770   URL http://ascelibrary.org/doi/10.1061/%28ASCE%29NH.1527-6996.0000220

771 Sassa, S., Takagawa, T., Jan. 2019. Liquefied gravity flow-induced tsunami: first evidence
772   and comparison from the 2018 Indonesia Sulawesi earthquake and tsunami disasters.
773   Landslides 16 (1), 195–200.
774   URL http://link.springer.com/10.1007/s10346-018-1114-x

775 Schmidtlein, M. C., Wood, N. J., Jan. 2015. Sensitivity of tsunami evacuation modeling to
776   direction and land cover assumptions. Applied Geography 56, 154–163.
777   URL https://linkinghub.elsevier.com/retrieve/pii/S0143622814002690

778 Soule, R. G., Goldman, R. F., May 1972. Terrain coefficients for energy cost prediction.
779   Journal of Applied Physiology 32 (5), 706–708.
780   URL https://www.physiology.org/doi/10.1152/jappl.1972.32.5.706

Tobler, W., 1993. Three Presentations on Geographical Analysis and Modeling: Non-Isotropic Geographic Modeling; Speculations on the Geometry of Geography; and Global Spatial Analysis (93-1). University of California at Santa Barbara: National Center for Geographic Information and Analysis., 26.
URL https://escholarship.org/uc/item/05r820mz

Treiber, M., Hennecke, A., Helbing, D., Aug. 2000. Congested traffic states in empirical observations and microscopic simulations. Physical Review E 62 (2), 1805–1824.
URL https://link.aps.org/doi/10.1103/PhysRevE.62.1805

United State Census Bureau, 2020. QuickFacts: United States; Crescent City city, California; North Bend city, Oregon; Coos Bay city, Oregon. Tech. rep.
URL https://www.census.gov/quickfacts/fact/table/US, crescentcitycitycalifornia,northbendcityoregon,coosbaycityoregon/PST045219

Wang, H., Mostafizi, A., Cramer, L. A., Cox, D., Park, H., Mar. 2016. An agent-based model of a multimodal near-field tsunami evacuation: Decision-making and life safety. Transportation Research Part C: Emerging Technologies 64, 86–100.
URL https://linkinghub.elsevier.com/retrieve/pii/S0968090X15004106

WGS, 2021. Tsunami Hazards in Washington State. Tech. rep., Washtington Geological Survey, Washington State Department of Natural Resources.
URL https://www.dnr.wa.gov/publications/ger_tsunami_hazards_brochure.pdf

Witter, R. C., Zhang, Y., Wang, K., Priest, G. R., Goldfinger, C., Stimely, L. L., English, J. T., Ferro, P. A., 2011. Simulating tsunami inundation at Bandon, Coos County, Oregon, using hypothetical Cascadia and Alaska earthquake scenarios. Tech. Rep. Special Paper 43, Oregon Department of Geology and Mineral Industries.
URL https://www.oregongeology.org/tsuclearinghouse/resources/sp-43/SP-43_onscreen144dpi.pdf

Wood, M. M., Mileti, D. S., Bean, H., Liu, B. F., Sutton, J., Madden, S., Jun. 2018. Milling and public warnings. Environment and Behavior 50 (5), 535–566.
URL http://journals.sagepub.com/doi/10.1177/0013916517709561

Wood, N. J., Jones, J., Spielman, S., Schmidtlein, M. C., Apr. 2015. Community clusters of tsunami vulnerability in the US Pacific Northwest. Proceedings of the National Academy of Sciences 112 (17), 5354–5359.
URL http://www.pnas.org/lookup/doi/10.1073/pnas.1420309112

Wood, N. J., Schmidtlein, M. C., Jun. 2012. Anisotropic path modeling to assess pedestrian-evacuation potential from Cascadia-related tsunamis in the US Pacific Northwest. Natural Hazards 62 (2), 275–300.
URL http://link.springer.com/10.1007/s11069-011-9994-2

Youd, T. L., Perkins, D. M., Apr. 1978. Mapping Liquefaction-Induced Ground Failure Potential. Journal of the Geotechnical Engineering Division 104 (4), 433–446.
URL http://ascelibrary.org/doi/10.1061/AJGEB6.0000612